ELSEVIER

Ceramics International 28 (2002) 521–526

CERAMICS INTERNATIONAL

www.elsevier.com/locate/ceramint

Nonlinear electrical properties of SnO_2·Li_2O·Ta_2O_5 varistors☆

C.P. Li[a], J.F. Wang[a,*], W.B. Su[a], H.C. Chen[a], W.X. Wang[a], G.Z. Zang[a], L. Xu[b]

[a]*Department of Physics, Shandong University, Jinan 250100, PR China*
[b]*Experiment Center, Shandong University, Jinan 250100, PR China*

Received 10 September 2001; received in revised form 6 November 2001; accepted 12 December 2001

Abstract

The electrical properties of (Ta, Li)-doped SnO_2 ceramics as a new varistor material were investigated. The sample 98.90% SnO_2·1.0% Li_2O·0.10% Ta_2O_5 (mol fraction) sintered at 1500 °C possesses the highest density ($\rho = 6.63$ g/cm^3) and nonlinear electrical coefficient ($\alpha = 10.8$). Effect of dopants and sintering temperature on the properties of the samples were investigated. The substitution of Sn^{4+} with Li^+ and the variation of sintering temperature play very important effects on the densities, dielectric constant, nonlinear electrical properties and other characteristics of the samples. The samples sintered at 1500 °C exhibit better physical and electrical properties than the samples sintered at 1400 °C. The properties of the grain-boundary defect barriers and the microstructural characteristics were investigated to ensure the effect of the dopants and the sintering temperature. A grain-boundary defect barrier model was used to illustrate the grain boundary barrier formation in SnO_2·Li_2O·Ta_2O_5 varistors. PACS numbers: 74.40.Lq; 72.20.Ht

Keywords: C. Electrical properties; E. Varistors; Tin oxide; Lithium oxide; Defect barriers

1. Introduction

Varistors are electric devices whose primary function is to sense and limit transient voltage surges and to do so repeatedly without being destroyed. The most important property of a varistor is its nonlinear current-voltage characteristic, which can be expressed by the equation $I = KV^{\alpha}$, where α is the nonlinear coefficient, a vital parameter used to scale the nonlinearity. The greater the value of α, the better the device.

Commercial varistors used in protection systems are based on SiC or on ZnO. Varistors based on ZnO, which exhibit good nonlinearity electrical properties, have been most extensively studied [1–3]. Varistors based on other ceramic systems are also under investigation, because of the need for even better properties.

Tin dioxide (SnO_2) is an *n*-type semiconductor with the rutile structure. It is characterized by low densification during sintering, an advantage for gas sensors [4]. Dense SnO_2-based ceramics can be achieved by introducing dopants or by hot isostatic pressure processing [5]. Pianaro reported that dopants with valence +2 could substitute for tin ions and create defects in the crystalline lattice, which will promote densification of SnO_2 ceramics [6]. The processing of SnO_2 based material with high-density enables its use in other types of electronic devices such as varistors, as reported by Pianaro et al. [6].

The alkali metal ion (Li^+) with valence +1 and ionic radius similar to that of Sn^{4+} can substitute the tin ions whose ionic radius is analogous to cobalt oxide. The objective of this work is to study the effect of Li_2O and the sintering temperature on Ta-doped SnO_2 varistor ceramics.

2. Experimental procedure

The raw chemicals in the present study were analytical grade SnO_2 (99.5%), Li_2CO_3 (99.9%) and Ta_2O_5 (99.95%). The following compositions have been investigated: $(100–0.10\text{-}X)\%SnO_2 + X\%Li_2CO_3 + 0.10\%\ Ta_2O_5$, where $X = 0.25$, 0.5, 1.0, 2.0. The chemicals were weighed and wet-milled in a polyethylene bottle with ZrO_2 balls for 14 h in deionized water and some

☆ Supported by the National Natural Science Foundation of China under grant No. 50072013.

* Corresponding author.
E-mail address: wangjf@sdu.edu.cn (J.F. Wang).

0272-8842/02/$22.00
PII: S0272-8842(02)00005-6

alcohol. The granulated powder was pressed into disks 15 mm in diameter and 1.5 mm in thickness at 160 Mpa, which were sintered at 1400 and 1500 °C for 1 h, then cooled to 800 °C at a constant rate of 5 °C/min. The green compacts were put into an Al_2O_3 crucible and fully surrounded with a powder of matching composition.

Apparent densities of the sintered samples were determined by Archimedes methods. For microstructural characterization, the samples were polished, thermally etched and analyzed in a scanning electron microscope (SEM) and the ceramic phases by X-ray diffraction (XRD). The mean grain sizes were determined by the intercept method. For electrical properties measurement, silver electrodes were made on both surfaces of the sintered pellets. The permittivities of the samples were investigated by using HP4192A LF Impedance Analyzer at 1 kHz. For electrical characterization of current density versus applied electrical field, a semiconductor I–V graph (QT2) was used.

3. Results

Fig. 1 shows the X-ray diffraction pattern of the composition doped with 1.0 mol% Li_2CO_3. There are no apparent second intergranular phases as in ZnO based varistors, but only the matrix of the SnO_2 rutile phase. The SEM micrographs show that the samples doped with 1.0 mol% Li_2O exhibit the largest grain size.

The nonlinear coefficient α was obtained by [7,8]

$$\alpha = \frac{\log(I_2/I_1)}{\log(V_2/V_1)} \tag{1}$$

where V_1 and V_2 are, respectively, the voltage at current I_1 and I_2. Fig. 1 shows I-V characteristics of the samples doped with different amounts of Li_2O sintered at 1400 and 1500 °C separately. It is found that the sample

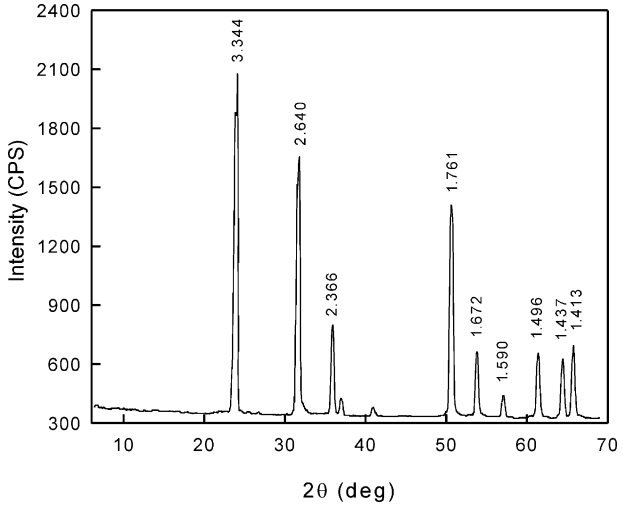

Fig. 1. X-ray diffraction patterns of the composition doped with 1.0 mol% Li_2CO_3 sintered at 1500 °C .

doped with 1.0 mol% Li_2O exhibits the highest nonlinear coefficient and the lowest reference electrical field. However, Fig. 1 shows that samples sintered at 1500 °C possess a higher nonlinear coefficient and a lower reference electrical field than samples sintered at 1400 °C. The reference voltage is proportional to the thickness of the pellet, which suggests that the non-ohmic behavior is a bulk property of SnO_2 ceramics, and not a property of the ceramic–electrode interface [9]. It is worthwhile to be figured out that the electrical properties of the samples remain almost unchanged during a long period or even after the annealing process.

Wang [10] developed a grain-boundary defect model for SnO_2-based varistors analogous to the band comprising the Schottky barriers. According to this model, the electric conduction in the ohmic region was associated with the thermion emission of the Schottky type. For this type of mechanism the current density is related to the electric field and temperature by the equation [10,11]:

$$J_s = A^* T^2 \exp[(\beta E^{1/2} - \phi_B)/kT] \tag{2}$$

where A^* is the Richardson's constant, ϕ_B is the interface voltage barrier height, E is the electric field and β is a constant related to the potential barrier width by the relationship:

$$\beta \propto 1/(r^*\omega) \tag{3}$$

where r is the number of grains per unit length and ω is the voltage barrier width.

Considering the Schottky type conduction model, plots of $\ln J$ against $E^{1/2}$ for the SnO_2 based varistor with various LiO_2 dopants sintered at 1400 and 1500 °C, as Fig. 2, can be built up at the low current density to determine the values for ϕ_B and β. The barrier height (ϕ_B) can be obtained from the intersection of the extrapolated lines of the plot with the voltage axis, and the relative magnitude of constant β, which is inverse to ω, can be derived from the slopes of the plots. Values of ϕ_B and ω are shown in Table 1. From Fig. 1, Table 1 and Table 2, we find that the highest and narrowest grain boundary voltage barrier occurs for the composition doped with 1.0 mol% Li_2O, which is consistent with its best nonlinear electrical properties. Table 1 also shows the variation of densities, electrical permittivities and shrinkage rates of samples sintered at 1400 and 1500 °C separately.

4. Discussion

4.1. Effect of dopants

Because there are no apparent secondary phases precipitated at the grain boundaries, defect formation by Li_2O and Ta_2O_5 in the SnO_2 matrix should be responsible

for the origin of the potential barriers at grain boundaries, which can also be used to explain the excellent stability of the samples. Thus, similar to the (Nb, Co) doped SnO_2 based varistor, the following equilibrium reaction may be written [11, 12]:

$$SnO_2 \longrightarrow Sn''_{Sn} + V_{\ddot{o}} + O_o^x + \frac{1}{2}O_2 \quad (4)$$

The addition of Ta_2O_5 in small amounts to the SnO_2 ceramics causes the concentration of e' and V_{sn}'''', which increase the electronic conductivity in the SnO_2 lattice and lead the semiconductivity of the grains according to:

$$Ta_2O_5 \xrightarrow{SnO_2} 2Ta_{\dot{Sn}} + 2e' + 4O_o^x + \frac{1}{2}O_2 \quad (5)$$

$$2Ta_2O_5 \xrightarrow{SnO_2} 4Ta_{\dot{Sn}} + V''''_{Sn} + 5O_2 \quad (6)$$

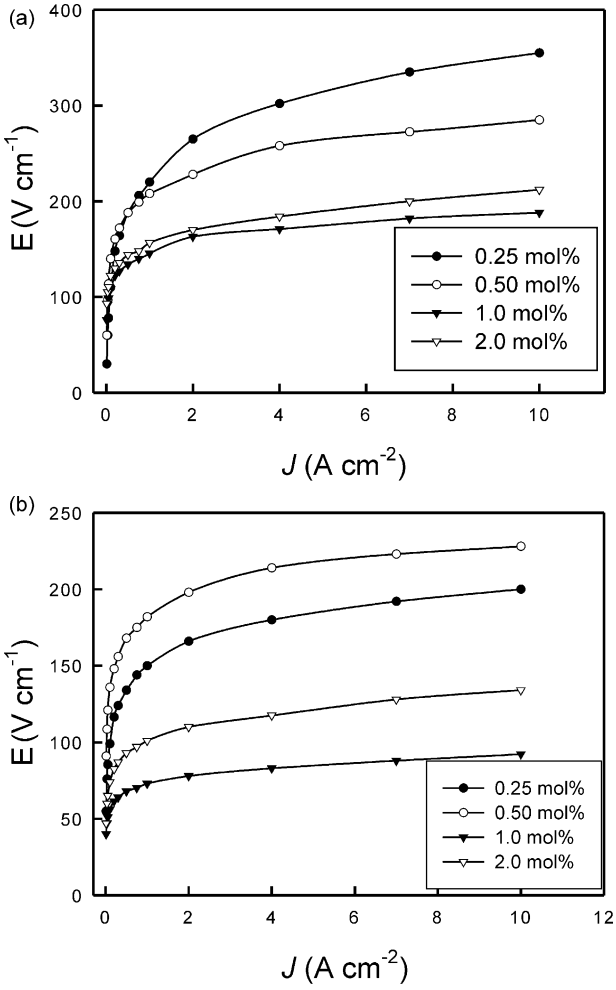

Fig. 2. I–V characteristics of samples with different Li_2CO_3 dopants sintered at 1400 °C (a) and 1500 °C (b).

Without the acceptor dopants, SnO_2 based ceramics exhibit no electrical nonlinearity because of the very low density. So unlike the TiO_2 based varistors, it is necessary for the acceptor dopants with the ionic radius similar to the SnO_2 lattice to increase the density of the samples. SnO_2 crystallizes in a tetragonal structure similar to rutile; there are interstitial sites that could accommodate foreign ions. Otherwise the ionic radius of Li^+ ($r = 0.068$ nm) is similar to the ionic radius of Sn^{4+} ($r = 0.071$ nm). These facts would facilitate the formation of oxygen vacancies and the formation of solid solution by substitutions or by interstitials [11], leading to the high densification of $SnO_2{\cdot}Li_2O{\cdot}Ta_2O_5$ system:

$$2Li_2O \xrightarrow{SnO_2} 2Li'''_{Sn} + 3V_{\ddot{o}} + O_2 \quad (7)$$

The oxygen vacancies can combine with tin vacancies according to the reaction:

$$2V_{\ddot{o}} + V''''_{Sn} \longrightarrow 2V_{\ddot{o}} + V''_{Sn} \quad (8)$$

Moreover, the increase of the concentration of oxygen vacancies induced by the substitution of Sn^{4+} with Li^+ will also play an important effect on the decrease of the grain resistivity because of an increased probability of electron hopping. Besides the substitution of Sn^{4+} with Li^+, Li^+ also tends to segregate to grain boundary areas, especially during cooling. The segregation of Li^+ and the diffusion of oxygen vacancies would increase the acceptor concentration (density of surface states, N_s) and then give high values of ϕ_B and ω through [13]:

$$N_s = 2\omega N_d \quad (9)$$

Table 1
Some characteristics of the samples with different amounts of Li_2CO_3 dopants sintered at 1400 °C

$LiCO_3$ (mol%)	α	d_r (g/cm^3)	Relative density (%)	V_B (V/mm)	ϕ_B	$\beta\times10^3$ (V$^{-1/2}$ cm$^{1/2}$)	ε_r (at 1 kHz)	Shrinkage rate
0.25	4.8	5.98	86.0	220.00	0.56	3.89	423.59	0.03
0.50	7.3	6.22	89.5	208.00	0.66	7.14	696.74	0.05
1.0	8.9	6.52	93.8	145.50	0.73	11.03	1082.57	0.10
2.0	7.6	6.85	98.6	156.50	0.71	8.05	210.72	0.13

Theoretical density of SnO_2, $d_t = 6.95$ g/cm^3.

$$\phi_B = q^2 N_s / 2\varepsilon_s N_d \quad (10)$$

$$\omega = (2\varepsilon_s \phi_B / q^2 N_d)^{1/2} \quad (11)$$

where N_d is donor density, q is electric charge and ε_s is the dielectric constant of the material.

It is shown by the former reactions that excess oxygen will be produced during the sintering process, which will provide the oxygen air for the sintering process as the result. The oxygen could also be responsible for Schottky barrier formation if we consider that oxygen can be adsorbed at the interfaces and react with negative defects according to [12]:

$$\frac{1}{2}O_2 \longrightarrow O_{ad}^{x} \quad (12)$$

$$2O_{ad}^{x} + V_{Sn}^{4-} \longrightarrow 2O^{-} + V_{Sn}^{2-} \quad (13)$$

$$2O_{ad}^{x} + Sn_{Sn}^{2-} \longrightarrow 2O^{-} + Sn_{Sn}^{x} \quad (14)$$

$$V_{Sn}^{4-} + 4O^{-} \longrightarrow 4O^{2-} + V_{Sn}^{x} \quad (15)$$

$$2O^{-} + Sn_{Sn}^{2-} \longrightarrow 2O^{2-} + Sn_{Sn}^{x} \quad (16)$$

The adsorbed oxygen at the grain boundary captures electrons from acceptor defects negatively charged at the grain boundary and stays at the interface, which facilitates the formation of Schottky barriers. Besides taking part in the formation of boundary barriers, the dopants of Sb^{3+} and Co^{2+} also create the sites to promote the adsorption of electrophylic species, O^- and O^{2-}, which further promote the nonlinearity of SnO_2 varistors accordingly.

Because the substitution of Sn^{4+} with Li^+ decreases the resistivity of grains, it will be beneficial for grain growth. Thus grain size increases with the amount of Li^+, as shown by SEM.

However, the substitution of Sn^{4+} with Li^+ and the segregation of Li^+ at the grain boundaries both exceed the maximum (1.0 mol%). If the dopant of Li^+ exceeds this limit, the extra Li^+ will concentrate in the interior of grains, which will block the formation and transportion of e^- and other defects. Thus, it will hinder the substitution and segregation of Li^+, which will impair the densification and the formation of the grain boundary barriers. The grain size also decreases accordingly. So the samples doped with 1.0 mol% Li_2O exhibit the highest densities, the best nonlinear electrical properties and the largest grain size.

According to the boundary barrier model, the reference voltage barrier, V_B, for a varistor is determined by the mean number of barriers $\overline{n}$ in series multiplied by v_b, that is [14]:

$$V_B = \overline{n}.v_b, \quad (17)$$

where v_b is the voltage barrier at the grain boundary; $\overline{n}$ is in inverse proportion to the grain sizes. The sample doped with 1.0 mol% Li_2O, with the largest grain size, exhibits the lowest reference electrical field.

Table 1 shows that all samples have very high permittivity, which cannot be accounted for by either SnO_2 ($\varepsilon = 9.65$) or the intergranular materials. The high permittivity of the ceramic comes, as Matsuoka pointed out, from the fact that the resistivity of SnO_2 grains is much lower than that of the grain boundary layers, so the entire voltage is sustained across narrow intergranular regions and the polarization is large. The dielectric constant of the ceramic is then [15]:

$$\varepsilon = \varepsilon_B d / t_B \quad (18)$$

where ε_B is the internal permittivity of the barrier material, d is the size of the cube grains and t_B is the mean thickness of the insulation barrier. It is shown from Eq. (18) that the dielectric capacitance is proportional to d/t_B, which can be used to explain the permittivity of the samples doped with 1.0 mol% Li_2O which exhibit the largest sizes of grains and the narrowest grain boundary barriers show the highest permittivity. However, it is shown from Table 2 that the sample 97.90% SnO_2·2.0% Li_2O·0.10% Ta_2O_5 sintered at 1500 °C exhibits an abnormally higher permittivity than the sample doped with 1.0 mol% Li_2O. The reason needs to further investigated.

4.2. Effect of sintering temperature

It is believed that the increase of the sintering temperature facilitates the transport of e^- and other defects,

Table 2
Some characteristics of the samples with different amounts of Li_2CO_3 dopants sintered at 1500 °C

$LiCO_3$ (mol%)	α	d_r (g/cm^3)	Relative density (%)	V_B (V/mm)	ϕ_B	$\beta \times 10^3$ (V$^{-1/2}$ cm$^{1/2}$)	ε_r (at 1 kHz)	Shrinkage rate
0.25	8.0	6.12	88.1	150.00	0.64	5.07	575.35	0.04
0.50	9.8	6.38	91.8	182.00	0.72	9.20	661.11	0.07
1.0	10.8	6.63	95.4	73.50	0.77	12.81	1239.79	0.13
2.0	8.1	6.86	98.7	101.50	0.73	7.51	1625.17	0.15

Theoretical density of SnO_2, $d_t = 6.95$ g/cm^3.

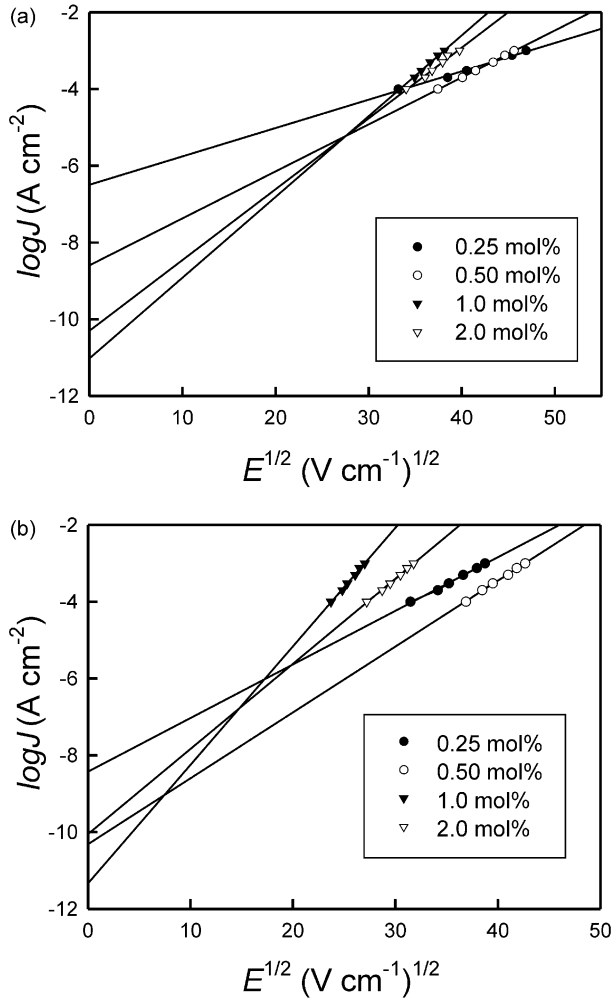

Fig. 3. Characteristic plots of $\ln J \times E^{1/2}$ for samples with different Li_2CO_3 dopants sintered at 1400 °C (a) and 1500 °C (b).

which is beneficial for the sintering process. Thus, with the increase of the sintering temperature, the densities, shrinkage rate and grain size increase accordingly. The increase of sintering temperature also facilitates the formation of grain boundary barriers, which make the samples sintered at 1500 °C exhibit the better nonlinear electrical properties, as shown in Table 2. The samples sintered at 1500 °C possessing the larger grain size and narrower grain boundary barriers exhibit the lower reference electrical field and higher permittivity than the samples sintered at 1400 °C, as shown in Table 1. Because Li_2O dopant exhibits a relative low melting point, it tends to evaporate at the high sintering temperature. The more the Li_2O dopant and the higher the sintering temperature, the more the amount of the evaporation. Thus the density of 97.90% SnO_2·2.0% Li_2O·0.10% Ta_2O_5 sample sintered at 1500 °C remains almost unchanged relative to the sample sintered at 1400 °C.

In contrast with Na^+ ($r = 0.093$ nm), Li^+ possesses similar ionic size to that of Sn^{4+}, which, together with

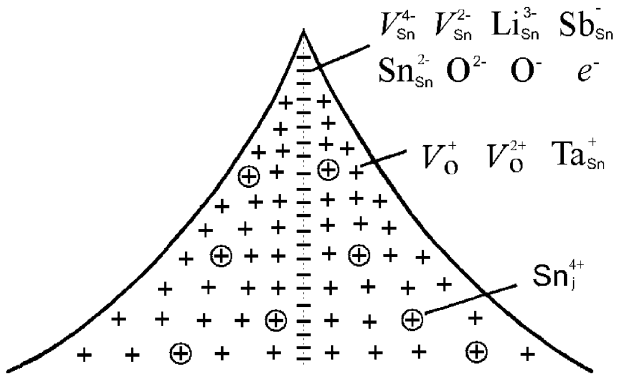

Fig. 4. The grain-boundary defect barrier model for SnO_2·Li_2O·Ta_2O_5 varistors.

the relative low melting point of Li_2O, will facilitate the substitution of Sn^{4+} more effectively. Thus, Li^+ doped samples exhibit the higher densities, better nonlinear properties and lower best-sintering temperature than the samples doped with Na^+.

4.3. Barriers model

Gupla and Carlson developed a grain boundary defect model for ZnO varistors analogous to the band model comprising the Schottky barrier [16]. In order to illustrate the grain boundary barrier formation in SnO_2·Li_2O·Ta_2O_5 varistors, an analogy to this model can be considered. In Figs. 3 and 4, the positively charged donors (V_o^{2+}, V_o^{+}, Ta_{Sn}^{+}, Sn_j^{4+}) extending from both sides of a grain boundary are compensated by the negatively charged acceptors (V_{Sn}^{4-}, V_{Sn}^{2-}, Li_{Sn}^{3-}, Sn_{Sn}^{2-}, O^{2-}, O^{-}, e^{-}) at the grain boundary interfaces, which form the depletion layers. Since a new phase precipitation in the grain boundary is not detected, the two barrier tops touch each other. One of the distinct characteristics of depletion layers is the asymmetric distribution of the internal ions as the out-of-order layers, which leads to the formation of voltage barriers for the electric transport. This transport occurs by tunneling and is responsible for the nonlinear ohmic characteristics [17].

5. Conclusions

The main conclusions are as follows:

1. The substitution and the segregation of Li^+ facilitate the sintering process and formation of grain boundary barriers. The samples doped with 1.0 mol% Li_2O exhibits the highest densities, the best nonlinear electrical properties and the highest permittivities.
2. Samples sintered at 1500 °C exhibit the better physical and electrical properties than samples sintered at 1400 °C.

3. In order to illustrate the grain boundary barriers formation in $SnO_2{\cdot}Li_2O{\cdot}Ta_2O_5$ varistors, a grain-boundary defect barrier model was developed.

References

[1] T. Asokan, Characterization of spinel particles in zinc oxide varistors, J. Mater. Sci. 25 (1990) 2447–2453.

[2] M. Matssuoka, Nonohmic properties of zinc oxide ceramics, Jpn. J. Appl. Phys. 10 (1971) 736–746.

[3] P.R. Emtage, The physics of zinc oxide varistors, J. Appl. Phys. 48 (1977) 4372–4384.

[4] J.G. Fagan, V.R.W. Amarakoon, Reliability and reproducibility of ceramic sensors: part III, huminity sensors, Am. Ceram. Soc. Bull. 72 (1993) 119–130.

[5] S.J. Park, K. Hirota, H. Yamamura, Enhanced sintering of tin dioxide with additives under isothermal condition, Ceram. Int. 10 (1984) 115–116.

[6] S.A. Pianaro, A new SnO_2-based varistor system, J. Mater. Sci. Lett. 14 (1995) 692–694.

[7] J.F. Wang, Nonlinear electrical behaviour of the $TiO_2{\cdot}Sb_2O_3$, Chin. Phys. Lett. 17 (2000) 530–531.

[8] T.K. Gopta, Application of zinc oxide varistors, J. Am. Ceram. Soc. 73 (1990) 1817–1840.

[9] V. Makarov, M. Trontelj, Novel varistor material based on tungsten oxide, J. Mater. Sci. Lett. 13 (1994) 937–939.

[10] Y.J. Wang, J.F. Wang, C.P. Li, Improved varistor nonlinearity via sintering and acceptor impurity doping, Eur. Phys. J. AP 11 (2000) 155–158.

[11] S.A. Pianaro, P.R. Bueno, E. Longo, J.A. Varela, Electrical properties of the SnO_2-based varistor, J. Mater. Sci. Mater. Electr. 9 (1998) 159–165.

[12] E.R. Leite, A.M. Nascimento, P.R. Bueno, E. Longo, J.A. Varela, The influence of sintering process and atmosphere on the non-ohmic properties of SnO_2 based varistor, J. Mater. Sci. Mater. Electr. 10 (1999) 321–327.

[13] J.J. Cheng, J.M. Wu, Effect of powder characteristics on electrical properties of (Ba, Bi, Nb)-added TiO_2 ceramics, Jpn. J. Appl. Phys. 35 (1996) 4704–4710.

[14] S.A. Pianaro, Effect of Bi_2O_3 addition on the microstructure and electrical properties of the SnO_2–CoO–Nb_2O_5 varistor system, J. Mater. Sci. Lett. 16 (1997) 634–638.

[15] J.M. Wu, C.J. Chen, Dielectric properties of (Ba,Nb) doped TiO_2 ceramics: migtation mechanism and roles of (Ba, Nb), J. Mater. Sci. 23 (1988) 4157–4164.

[16] T.K. Gopta, W.D. Carlson, A grain-boundary defect model for instability/ stability of a ZnO varistor, J. Mater. Sci. 20 (1985) 3487–3500.

[17] Y.J. Wang, Electrical properties of (Zn,Nb)-doped SnO_2 varistor system, J. Phys. D: Appl. Phys. 33 (2000) 96–99.